J Neurophysiol 99: 1857–1870, 2008.
First published January 23, 2008; doi:10.1152/jn.00119.2007.

The Effects of Microstimulation of the Dorsomedial Frontal Cortex on Saccade Latency

Shun-nan Yang,[1,2] Stephen J. Heinen,[1] and Marcus Missal[3]

[1]*Smith-Kettlewell Eye Research Institute, San Francisco, California;* [2]*Vision Performance Institute, College of Optometry, Pacific University, Forest Grove, Oregon; and* [3]*Laboratoire de Neurophysiologie, Université Catholique de Louvain, Brussels, Belgium*

Submitted 2 February 2007; accepted in final form 23 January 2008

Yang S, Heinen SJ, Missal M. The effects of microstimulation of the dorsomedial frontal cortex on saccade latency. *J Neurophysiol* 99: 1857–1870, 2008. First published January 23, 2008; doi:10.1152/jn.00119.2007. Neural regions in the dorsomedial frontal cortex (DMFC), including the supplementary eye field (SEF) and the presupplementary motor area (pre-SMA), are likely candidates for generating top-down control of saccade target selection. To investigate this, we applied electrical microstimulation to these structures while saccades were being planned to visual targets. Stimulation administered to superficial and lateral DMFC sites that were within or close to the SEF delayed ipsilateral and facilitated contralateral saccades. Facilitation was limited to saccades made toward targets in a narrow, contralateral movement field that had endpoints consistent with the goal of evoked saccades. Facilitation occurred with current delivered before target onset and delay with current applied after this time. Stimulation at deeper, medial sites that encompassed the pre-SMA resulted in mostly bilateral delay. The amount of delay at these sites was usually greater for ipsilateral saccades and increased with current amplitude. Changes in saccade latency were not accompanied by altered endpoint, trajectory, or peak velocity. The spatial specificity of SEF stimulation in inducing latency changes suggests that the SEF participates in selecting saccade goals. The less specific delay with pre-SMA stimulation suggests that it is involved in postponing visually guided saccades, thus likely permitting other oculomotor structures to select saccade goals.

INTRODUCTION

Primates use rapid eye movements, or saccades, to extract detailed information from visual scenes with the fovea (Leigh and Zee 2006; Wurtz and Goldberg 1989). When multiple objects are present that compete to be the target, a selection process is necessary (Arai and Keller 2005; Arai et al. 1994; Findlay and Walker 1999). Recent studies have shown that neural activity in many oculomotor regions evolves to signal which of competing targets will be selected [e.g., superior colliculus (SC): Li and Basso 2005; McPeek and Keller 2002, 2004; the frontal eye field (FEF): Thompson et al. 1996; and the basal ganglia: Basso and Wurtz 2002]. It is currently not clear, however, whether these are the areas making the selection or whether their activity reflects selection made by other areas.

Regions in the dorsomedial frontal cortex (DMFC), including the supplementary eye field (SEF) (Schlag and Schlag-Rey 1987) and the presupplementary motor area (pre-SMA) (Isoda 2004; Isoda and Hikosaka 2007; Isoda and Tanji 2002; Tanji 2001), might be good candidates for influencing saccade target selection. The SEF is located in the lateral DMFC, between the midline and the genu of the arcuate sulcus (for reviews, see Schall 1991; Tehovnik 1995). The SEF has direct connections to the SC (Fries 1985) and the brain stem (Hartmann-von Monakow et al. 1979; Shook et al. 1998, 2000), and low-current microstimulation here evokes contralateral saccades (Martinez-Trujillo et al. 2003; Park et al. 2005; Russo and Bruce 2000; Schiller and Chou 1998; Schlag and Schlag-Rey 1987; Tehovnik 1995; Tehovnik and Lee 1994). Some SEF neurons show heightened activity during countermanding (Stuphorn et al. 2000) and go/no-go tasks (Schall 1991), in which a visually guided saccade must be withheld based on task cues. SEF neurons are also active in the antisaccade task, in which a visually guided ipsilateral saccade is replaced with an endogenously generated contralateral one (Amador et al. 2004; Schlag-Rey et al. 1997). These findings suggest that the SEF plays a supervisory role in saccade generation (Schall et al. 2002) and may be involved in selecting between competing saccades plans.

Recent studies have shown that the pre-SMA, situated medial and ventral to the SEF, is also involved in top-down control of saccade initiation (Hoshi and Tanji 2004; Isoda 2004; Isoda and Tanji 2004; Nachev et al. 2005; Tanji 2001). This region does not have direct connections to the SC or the brain stem (Fries 1987; Hartmann-von Monakow et al. 1979), and stimulating here does not evoke saccades (Fujii et al. 2002). Rather, stimulation in the pre-SMA results in greater ipsilateral than contralateral delay (for observed facilitation effect, see Isoda 2004). Moreover, some pre-SMA neurons are more active when saccades are directed toward a newly cued location, compared with when saccades are made to the same location but without a change of cued location (Isoda and Hikosaka 2007). These results implicate the pre-SMA in supervising the selection of saccade targets, but not in directly triggering them.

The above-cited findings suggest that both areas are good candidates to participate in target selection. However, no studies have directly compared them in this regard, although they have been compared with respect to their roles in saccade planning (Fujii et al. 2002), and in resolving competing voluntary saccade plans (Nachev et al. 2005). To assess the specific contributions of the SEF and pre-SMA to saccade target selection, we applied electrical microstimulation to each structure around the time when visually guided saccades were being planned. Our rationale was that if a region participates in saccade target selection by signaling a preferred target location, the command elicited by stimulation should compete or

Address for reprint requests and other correspondence: S. Heinen, 2318 Fillmore Street, San Francisco, CA 94115 (E-mail: heinen@ski.org).

The costs of publication of this article were defrayed in part by the payment of page charges. The article must therefore be hereby marked "*advertisement*" in accordance with 18 U.S.C. Section 1734 solely to indicate this fact.

cooperate with the saccade being planned to the visual target, and therefore either facilitate or inhibit that saccade.

METHODS

Subjects and surgical procedures

Three juvenile male macaque monkeys (GU, CL, and VC) participated in the experiments. One of them (GU) was involved in an earlier smooth pursuit study (Missal and Heinen 2004), in which anticipatory pursuit facilitation was obtained from stimulating the DMFC. Surgeries were performed under aseptic conditions to implant a recording chamber, head holder, and a search coil to measure eye movements. With the monkey under isoflurane gas anesthesia, a 2-cm craniotomy was trephined in the skull. The chambers implanted on the monkeys were centered 24 mm anterior in Horsley–Clarke stereotaxic coordinates for GU and VC, and 24 mm anterior and 7.5 mm to the right for CL. A stainless steel recording chamber with an inner diameter of 1.4 cm was positioned over the craniotomy. The eye coil, constructed from Teflon-coated stainless steel wire, was implanted under the conjunctiva of one eye (Judge et al. 1980). The head holder was positioned on the midline. After surgery, the monkey was returned to its cage and allowed to recover fully before experiments began. Antibiotics and analgesics were administered under the direction of a veterinarian during the postoperative period. All procedures were approved by the California Pacific Medical Center Institutional Animal Care and Use Committee and were in compliance with the guidelines set forth in the U.S. Public Health Service Guide for the Care and Use of Laboratory Animals.

Experimental procedures

Stimulation was delivered through tungsten microelectrodes of 85–100 mm length (FHC) that were lowered to sites in the DMFC through a stainless steel guide tube. The impedance of each electrode at the beginning of each session was 1.0–2.0 MΩ; at the end of each session the impedance usually dropped significantly, often to <0.3 MΩ. The stimulation trains consisted of biphasic pulses with a duration of 0.2 ms for each phase; the stimulation frequency was set at 300 Hz and pulse-train duration was usually 100 ms. These parameters provided the optimal change in saccade latency with low current. The current amplitude was set just above the threshold for causing a latency change, typically between 50 and 75 μA. For some sites, we varied stimulation duration (50–500 ms), current amplitude (25–600 μA), and target onset asynchrony (TOA) (−75 to +150 ms).

Monkeys were trained to make saccades to a 0.5° white spot that appeared at horizontal locations 10° to the left or right of the fixation point. Each trial began with the appearance of a fixation point at the center of the screen. The monkey had to acquire the fixation point and maintain fixation within a 3° window centered on it for 500 ms, after which time the fixation point was extinguished and a target was displayed peripherally at either horizontal location. After the target appeared, the monkey had 500 ms to acquire it and had to maintain fixation within a 4° window centered on it for an additional 500 ms. Liquid reward was given if the monkey successfully performed the trial. The intertrial interval was variable but always exceeded 400 ms.

In each experimental session, stimulation with −25-ms TOA and 75-μA current amplitude was first applied to search for effective facilitation sites along an electrode track. Stimulation with +75-ms TOA was then used to search the same track for delay sites. If an effect was found with either a −25- or +75-ms TOA, the other TOA was used to test the same site. Each site was categorized based on the type of initial effect. For example, if there was significant ipsilateral delay and contralateral facilitation with a −25-ms TOA, the site was classified as "−con/+ipsi," regardless of the effect later obtained with +75-ms TOA. When an effective site was found, the threshold current for affecting saccade latency was determined and the stimulation parameters and target locations were varied when necessary. Single-unit activity close to the effective site was recorded from neurons at some sites while the monkey was making saccades to targets 10° away from the fixation point horizontally or vertically. Only the activity of neurons isolated within 100 μm of the optimal depth for the stimulation effect was recorded and analyzed. The difference in neural signals was mostly moderate in response to targets appearing at the contralateral and ipsilateral locations.

Due to the time limit of each experimental session, typically only one stimulation parameter was systematically manipulated at a site. In addition, in some sessions after a site was found, target position was manipulated to investigate the spatial tuning of the stimulation effect, with the threshold current amplitude and two TOAs (−25 and +75 ms). The target appeared at one of three eccentricities (5, 10, 15°) and one of 12 equally spaced radial angles; either one TOA or both TOAs were used in a single session depending on the session's duration. At effective sites we attempted to evoke saccades, while the monkey was in the dark, with the same threshold current used to alter saccade latency.

Data analysis

Effective stimulation sites were determined by on-line visualization of single and averaged eye position traces for stimulation and control trials. Vertical and horizontal eye position signals were digitized (1 kHz) and stored for off-line analysis. Eye velocity was obtained by digital differentiation with a filtering cutoff frequency of 50 Hz. Saccade onset was detected using a velocity threshold of 40°/s. Saccade landing error was obtained by computing the distance between target position and saccade endpoint. Maximum trajectory deviation was defined as the largest angular separation between a straight line that connected initial eye position and the target location, and a straight line that connected initial eye position and momentary eye position. Peak velocity was defined as the maximum radial eye velocity during the saccade.

To compare the magnitude of a given stimulation effect with various parameters and TOAs at different sites, we computed a *t*-value for the difference in saccade latency between control and stimulated trials. The mean latency obtained from control trials at each site was subtracted from that obtained from stimulated trials at the same site, and the difference in means was normalized against the SE of the difference. A *t*-value ≥1.96 indicates a significant difference.

Directional tuning of neural activity at stimulation sites was measured using the following procedure. Neural activity was recorded while the monkey was planning a saccade to a target that appeared at one of four locations (10° up, down, left, and right of the central fixation point). A directional index (DI) was then derived from the vector sum of normalized mean spike rate for the 100 ms prior to saccade initiation. The mean spike rate for the four target locations was normalized against that for the location having the highest mean spike rate.

Gaussian curve fitting was implemented to compare the directional tuning of the stimulation effect across different types of stimulation sites. The location with the maximum latency change was first identified and the mean latency change for each target location of the same eccentricity was then normalized against the maximal latency change. A least-squares method was used to obtain the best fit. The SD of the curves for different stimulation sites was statistically compared using an *F*-test.

Matlab and its Signal Processing and Statistical Toolboxes (The MathWorks, Natick, MA) were used to implement all data analysis algorithms. The Matlab Statistics Toolbox and SPSS 13.0 (SPSS, Chicago, IL) were used to perform postexperimental statistical analyses. The significance of all observed effects underwent a *t*-test, with a statistical significance level (*P* value) set at 0.05.

Histology

After completion of the experiments, the monkeys were perfused and the brains were fixed with 10% formalin. For monkey VC,

5-μm-thick coronal slices were taken from the DMFC and stained (hematoxylin-and-eosin and Perl) to highlight the electrode tracks. In addition, before perfusing monkey VC, two electrical lesions were made with DC current located 2 mm laterally from the center of the chamber and 4.5 mm in depth. After perfusion, the reference lesions were revealed using cresyl violet staining. The recorded site depth and locations in experimental sessions were then aligned to these reference tracks.

RESULTS

Saccade delay and facilitation

Low-amplitude stimulation applied to 79 DMFC sites resulted in delay and/or facilitation of saccade initiation. Results from three example stimulation sites, obtained with current amplitudes of 50 to 75 μA and a duration of 100 ms, are shown

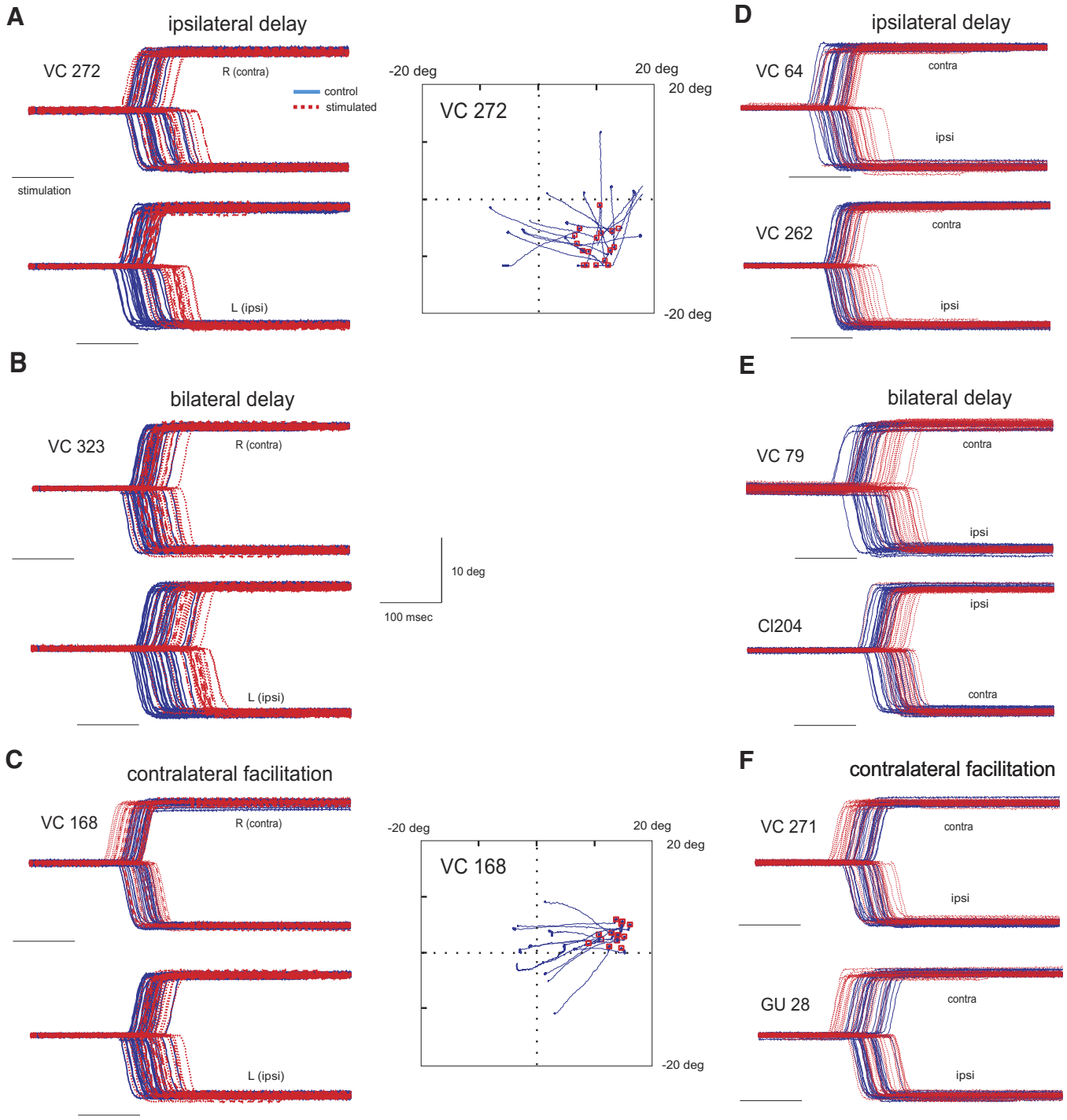

FIG. 1. Eye movements recorded from example dorsomedial frontal cortex (DMFC) sites. *A*, *left*: horizontal eye position recorded while stimulating site VC 272 with a −25- or a +75-ms target onset asynchrony (TOA), respectively (blue: control; red: stimulated). *Right*: horizontal and vertical eye position for saccades evoked at the same site while the monkey was in the dark (red square: saccade endpoint). *B*: horizontal eye traces recorded from site VC 323. *C*: eye traces recorded and evoked from site VC 168. *D*: additional horizontal eye traces obtained from 2 ipsilateral delay sites. *E*: additional eye traces from bilateral delay sites. *F*: additional eye traces from contralateral facilitation sites.

TABLE 1. *Summary of stimulation effects in the three monkeys in this study*

	Frequencies of Effective Sites					
	Horizontal targets (10°)		Site location		Multiple directions/ amplitudes	
Type of Effect	−25 ms	+75 ms	SEF	Pre-SMA	−25 ms	+75 ms
+ con	—	13 (0)	4	9	—	—
+ ipsi	4 (0)	20 (4)	20	4	2/2	6/6
+ con/+ ipsi	—	25 (0)	8	17	—	8/9
− con	11 (6)	—	10	1	5/11	0/2
− ipsi	2 (0)	—	2	—	—	—
− con/+ ipsi	4 (4)	—	4	—	2/4	0/2

Columns 2 and 3 show numbers of sites where initially facilitation (−) and/or delay (+) effects were found for ipsilateral (ipsi) or contralateral (con) 10° horizontal targets. A site was assigned to one of these cells, depending on the initial effect found there and the initial stimulation timing (TOA) used; later effects with other timings, durations, or amplitudes are not shown here (see METHODS and RESULTS). Empty cells indicate the type of effect was not found with the corresponding TOAs. Numbers of evoked saccade sites are in parentheses. Columns 4 and 5 summarize delay and facilitation sites for each structure. Columns 6 and 7 show sites in corresponding cells of columns 2 and 3 tested with multiple target locations. The denominator indicates the number of sites where all 36 target locations were tested; the numerator indicates sites where a significant effect was seen at one or more of the 36 target locations.

in Fig. 1. Figure 1*A* shows results obtained from an ipsilateral delay site (VC 272, depth = 1.2 mm, A/P = −2 mm, M/L = −3 mm) (by convention, negative numbers will be used to refer to posterior and left site locations). The left panels show the horizontal eye position for trials in which −25- (Fig. 1*A*, *top*) and +75-ms (Fig. 1*A*, *bottom*) TOAs were used for saccades made toward targets at the two 10° horizontal locations. The bars below the eye traces indicate the stimulation period. Stimulated (red traces) and unstimulated control trials (blue traces) were intermixed randomly in the same block of trials. The right panel shows horizontal and vertical eye position traces from saccades evoked at the same site with the same current amplitude, obtained while the monkey was in the dark (mean latency = 78 ms; SD = 14.2 ms). No facilitation or delay was found with −25-ms TOA (*top*; ipsilateral: +14 ms, $t = 1.65$, $P = 0.077$; contralateral: +8 ms, $t = 0.81$, $P = 0.23$); ipsilateral saccades were significantly delayed by stimulation using a +75-ms TOA (*bottom*), whereas contralateral saccades were not significantly affected (ipsilateral: +60 ms, $t = 61.75$, $P < 0.0001$; contralateral: +10 ms, $t = 1.94$, $P = 0.059$). Here "+" indicates delay and "−" facilitation. Figure 1*B* shows results obtained from a bilateral delay site (VC 323, depth = 2.6 mm, A/P = −1 mm, M/L = −2 mm). Here, ipsilateral saccades were delayed with a −25-ms TOA (*top*; ipsilateral: +29 ms, $t = 7.82$, $P = 0.0021$; contralateral: +12 ms, $t = 1.15$, $P = 0.13$); delay in both directions was found with a +75-ms TOA (*bottom*; ipsilateral: +47 ms, $t = 40.44$, $P < 0.0001$; contralateral: +23 ms, $t = 38.50$, $P < 0.0001$). Stimulating here with the same threshold current amplitude (75 μA) did not evoke saccades. Figure 1*C* shows results from a contralateral facilitation site (VC 168, depth = 2.4 mm, A/P = 1 mm, M/L = −3 mm), for which contralateral saccades were facilitated but ipsilateral saccades were unaffected with a −25-ms TOA (*top*; ipsilateral: +14 ms, $t = 0.06$, $P = 0.515$; contralateral: −30 ms, $t = -9.32$, $P < 0.01$). With a +75-ms TOA (*bottom*), ipsilateral delay was observed but there was no contralateral facilitation or delay (ipsilateral: +26 ms, $t = 6.27$, $P = 0.0076$; contralateral: +5 ms, $t = 0.52$, $P = 0.37$). Saccades were evoked from this site with a mean latency of 86 ms (SD = 16.3 ms). Figure 1, *D–F* shows additional examples of horizontal eye traces in stimulated and control trials obtained from ipsilateral delay (Fig. 1*D*), bilateral delay (Fig. 1*E*), and contralateral facilitation sites (Fig. 1*F*). Note that a site was categorized based *only* on the initial effect observed (with either −25- or +75-ms TOA), not other effects found later at the same site with a different TOA.

Table 1 reports the frequencies of stimulation sites where there was a significant latency change. Columns 2 and 3 show the number and type of sites from which delay or facilitation of 10° horizontal saccades was obtained with 50- to 75-μA current for all three monkeys. Again, we classified a site based solely on the initial effect observed because different TOAs often caused different types of effects for saccades in the same direction. For example, row 2 of columns 2 and 3 shows that stimulation at four sites initially caused ipsilateral delay with a

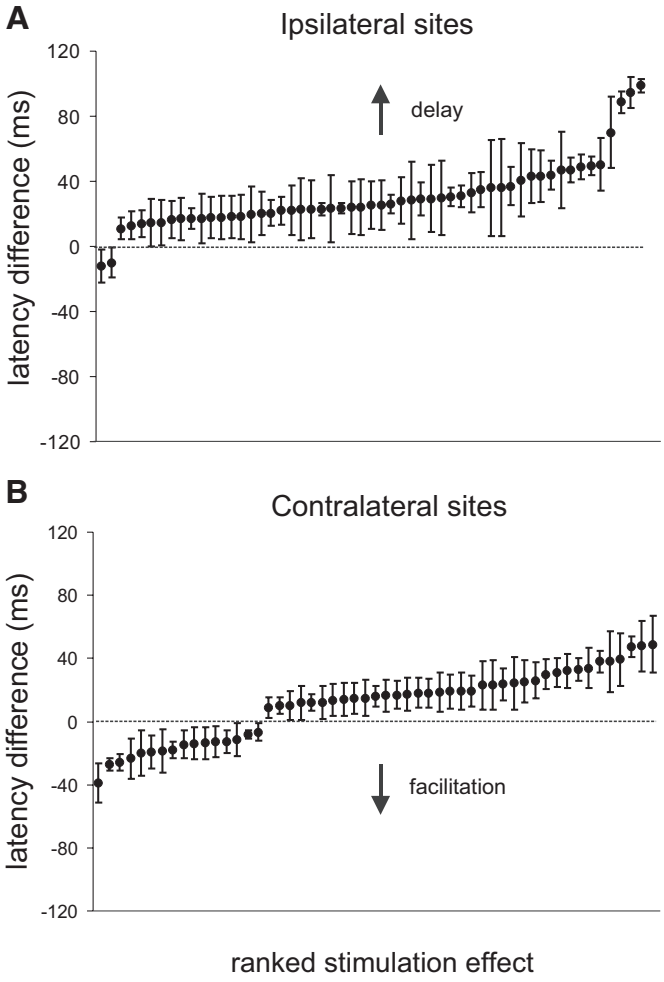

FIG. 2. Ranked magnitude of facilitation and delay effects from all monkeys. One or both directions of the 79 effective sites that had a significant latency change were included in the figure, resulting in 102 entries. All effects were obtained with 50- to 75-μA current. *A*: stimulation effect on ipsilateral saccades, sorted by effect direction (facilitation vs. delay) and magnitude (stimulated minus control). Error bars indicate 95% confidence intervals of the difference in saccade latency. *B*: stimulation effect on contralateral saccades.

−25-ms TOA. These sites were classified as "+ipsi" despite that later stimulation with a +75-ms TOA resulted in bilateral delay. There were also 20 sites where we initially found ipsilateral delay, but with a +75-ms TOA. These sites are classified as "+ipsi" as well. Overall, stimulation at 62 sites resulted in contralateral delay, ipsilateral delay, or both, with a −25- or a +75-ms TOA; 13 sites showed contralateral (12) or ipsilateral (1) facilitation with a −25-ms TOA; and 4 sites showed both contralateral facilitation and ipsilateral delay with a −25-ms TOA. Note that effects obtained from manipulating other stimulation parameters are not included here. Also in columns 2 and 3, numbers in parentheses indicate the number of sites out of the total number of sites in the same table cell at which saccades were evoked.

Figure 2 reports the ranked magnitude of stimulation effects for all significant sites, sorted according to the sign of the latency change (facilitation or delay) and the hemisphere where the site was found. Effects obtained for both horizontal target

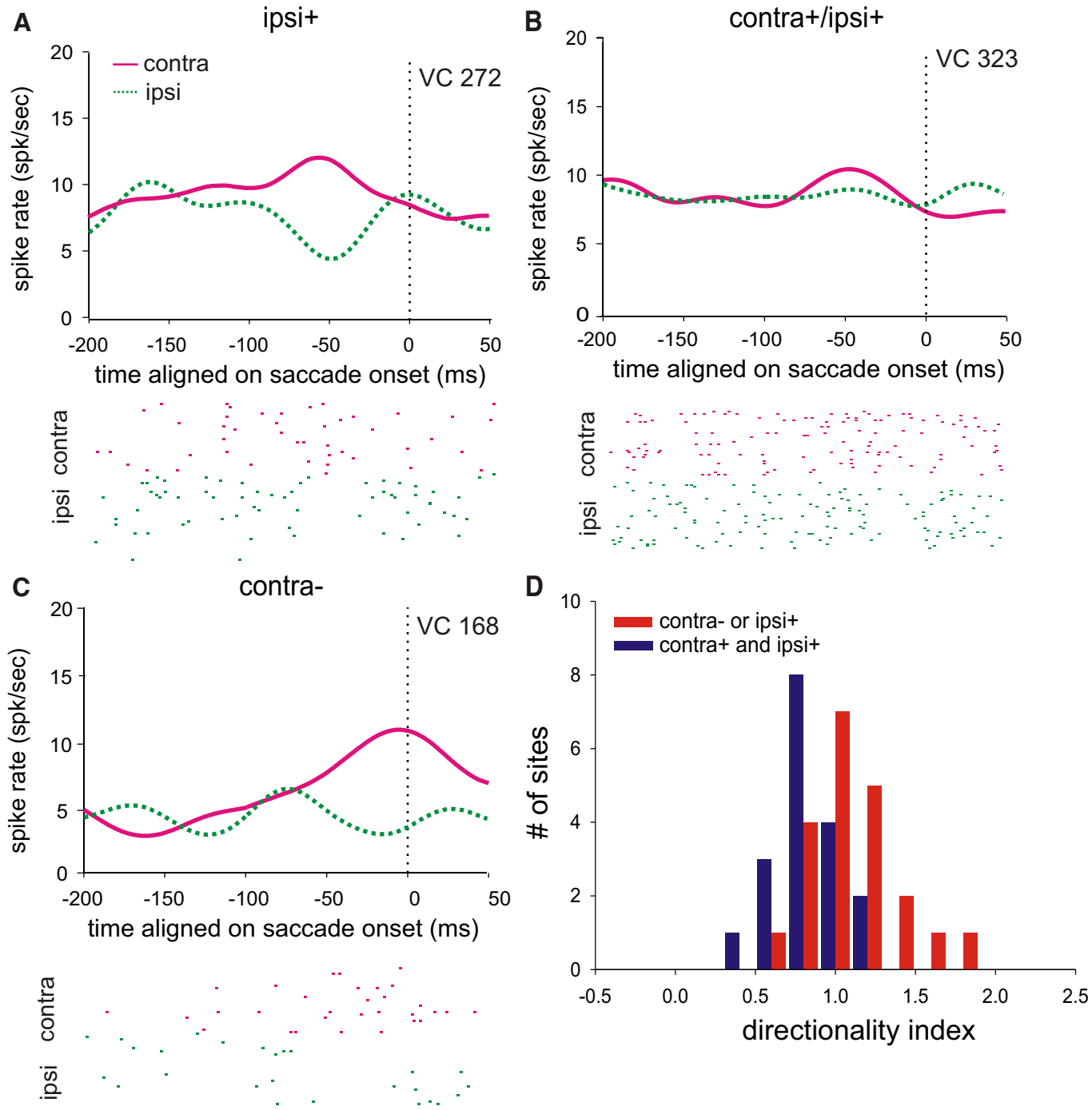

FIG. 3. Neural activity recorded close to facilitation and delay sites. *A*: activity from ipsilateral delay site VC 272. The target appeared at one of the 2 horizontal locations contralateral or ipsilateral to the recorded site; spikes were aligned with saccade onset. The dashed line indicates saccade onset time. *B*: neural activity recorded from bilateral-delay site VC 323. *C*: activity recorded from site VC 168. *D*: directional tuning of DMFC neurons recorded from bilateral delay sites and from ipsilateral delay or contralateral facilitation sites. A directional index (DI) ≥1 indicates strong tuning (see METHODS).

locations at the same site are shown as separate data points if both were significant. Overall, ipsilateral saccades were usually delayed. Contralateral saccades, although usually being delayed as well, were more often facilitated than ipsilateral ones. The mean delay for ipsilateral sites (32.1 ms) was significantly greater than that for contralateral ones (23.4 ms) [$t_{(53,55)} = 2.43$, $P = 0.017$].

At some sites, we recorded neuronal activity after a stimulation effect was found and before extensive stimulation was done. Figure 3, *A–C* shows activity recorded from the three

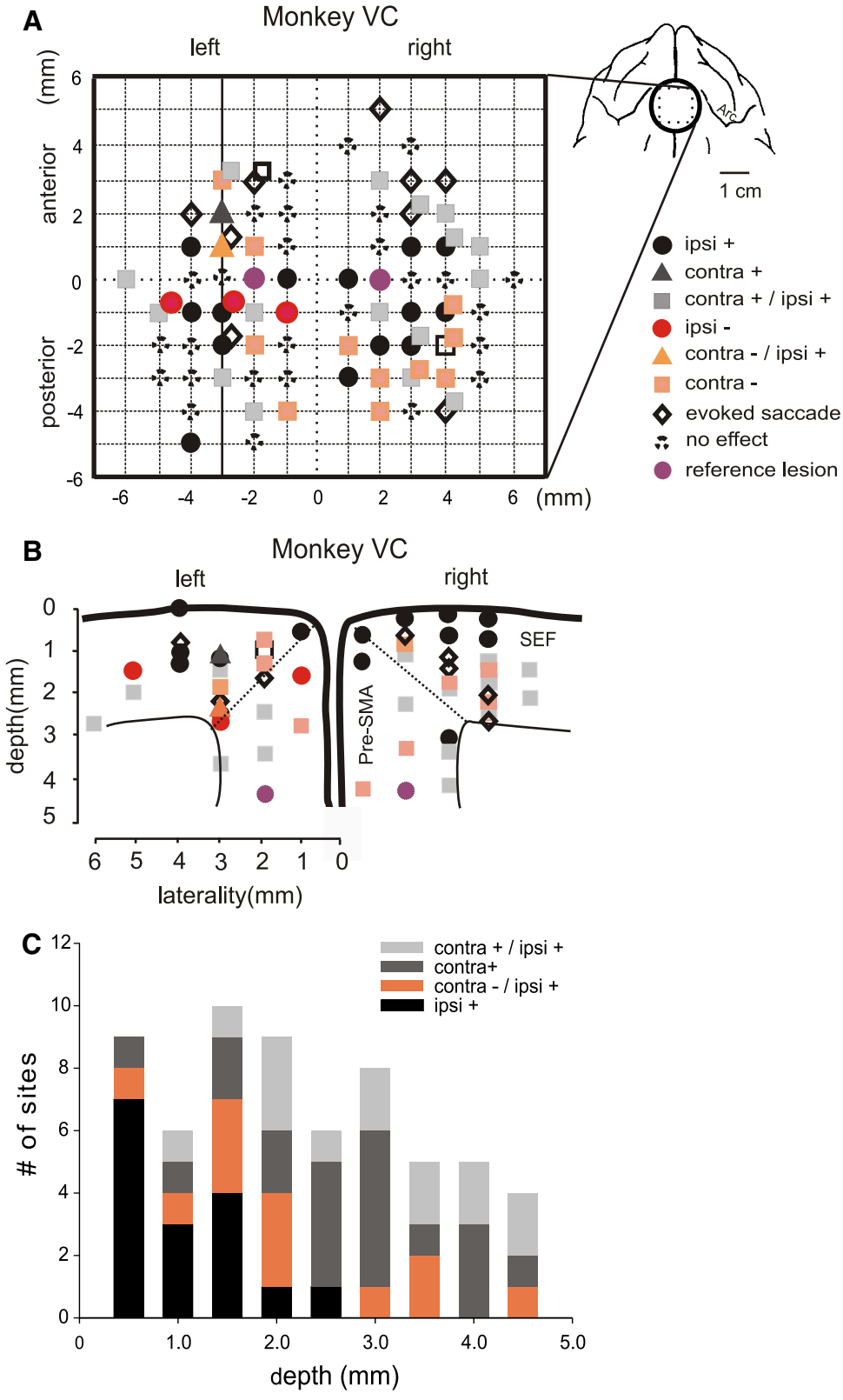

FIG. 4. Locations and depths of significant DMFC sites. *A*: topographic map of probed sites recorded from monkey VC. The center of the map corresponds to the center of the chamber, as indicated in the *inset* in the *top right* corner, which was 24 mm anterior and on the midline. Different effects are shown as different symbols. Saccade facilitation is indicated by a "−" and saccade delay is indicated by a "+" in the legend. Each electrode track was separated from adjacent tracks by 1 mm, but some tracks were probed more than once, as illustrated by symbols that are offset slightly. Positive *x*- and *y*-axis values indicate anterior and right locations; negative values indicate posterior and left. Reference lesions are marked with purple circles. The locations and depths of all sites from VC were aligned here in relation to the reference lesions. Evoked saccade sites are shown as diamonds. All effects and evoked saccades were obtained with 50–75 μA. *B*: horizontal positions and measured depths of stimulation sites recorded from monkey VC. The coronal schematic of probed sites is based on a reference histological slice from monkey VC, close to the center of the DMFC chamber. *C*: distributions of site depths for different stimulation effects for all 3 monkeys.

sites in Fig. 1. In Fig. 3*A*, the mean spike rate recorded from VC 272 (an ipsilateral delay site) was aligned to saccade onset, when the target appeared at 10° contralateral (magenta curve) or ipsilateral (green curve) horizontal locations. A presaccadic increase in activity occurred when the target appeared at the contralateral location and activity was suppressed for the ipsilateral target. Figure 3*B* shows no change in mean spike rate for the neuron recorded from site VC 323 where a bilateral delay was found with a +75-ms TOA. Presaccadic activity occurred for the contralateral target but not for the ipsilateral one at site VC 168, where contralateral facilitation was observed with a −25-ms TOA (Fig. 3*C*). Figure 3*D* shows histograms of directional index (DI) values that estimate the directional preference of neurons recorded at bilateral delay sites and at contralateral facilitation or ipsilateral delay sites (see METHODS). In general, neurons at ipsilateral delay or contralateral facilitation sites exhibited sharper directional tuning than that of neurons at bilateral delay sites.

Topography of stimulation sites

To characterize the topography of stimulation sites, we plotted the locations of the sites in monkey VC from which the most sites were obtained (Fig. 4*A*). Most sites where saccades were evoked were ≥3 mm from the midline, consistent with earlier findings (Park et al. 2005; Russo and Bruce 2000; Schlag and Schlag-Rey 1987; Tehovnik 1995); however, there is no clear topographic difference among the different types of sites.

Figure 4*B* shows the depths of the sites in Fig. 4*A*, collapsed onto a diagram of a coronal slice at the level of the reference lesions. The boundary of the SEF and the pre-SMA, as defined previously (Fujii et al. 2002), is delineated with dashed lines. The different effects are marked by the same symbols as those in Fig. 4*A*. The depth was measured as the distance the electrode traveled from where neuronal activity was first encountered to where the stimulation effect was obtained. The measured locations and depths were aligned to those of the reference lesions (depth = 4.5 mm). A summary of site frequency in relation to the SEF and the pre-SMA is reported in columns 4 and 5 of Table 1.

Figure 4*B* shows that most ipsilateral delay sites were located superficially within or close to the SEF, whereas bilateral delay sites were usually located within the pre-SMA or close to its boundary, and deep within the SEF. Note that all types of latency changes were observed in the SEF, but the effects obtained from pre-SMA stimulation were mostly bilateral. Figure 4*C* summarizes the mean depths of sites where facilitation and delay were obtained, for all sites from the three monkeys. The mean depths were 0.97 mm (ipsi+, SD = 0.25 mm), 2.1 mm (ipsi+/contra−, SD = 0.24 mm), 2.92 mm (ipsi+/contra+, SD = 0.27 mm), and 2.42 mm (contra+, SD = 0.22 mm), respectively. All three types of sites with bilateral effect were located deeper than ipsilateral ones (all $P < 0.05$).

Stimulation parameters

Differences in stimulation timing, current amplitude, and duration have been shown to affect saccade latency (Isoda 2004; Tehovnik 1995; Tehovnik and Lee 1993; Tolias et al. 2005). We systematically manipulated these parameters at some sites where latency effects were observed. Figure 5 reports the effect of varying TOA. Figure 5*A* shows the effect of stimulation with 65-μA current of 100-ms duration at one site (GU 26; depth = 2.2 mm, A/P = −2 mm, M/L = −3 mm), with TOAs between −75 and +125 ms. This site was chosen for its strong facilitation effect and because it was tested with the full set of TOAs. The ordinate indicates the difference in saccade latency between control and stimulated trials, where negative values correspond to facilitation and

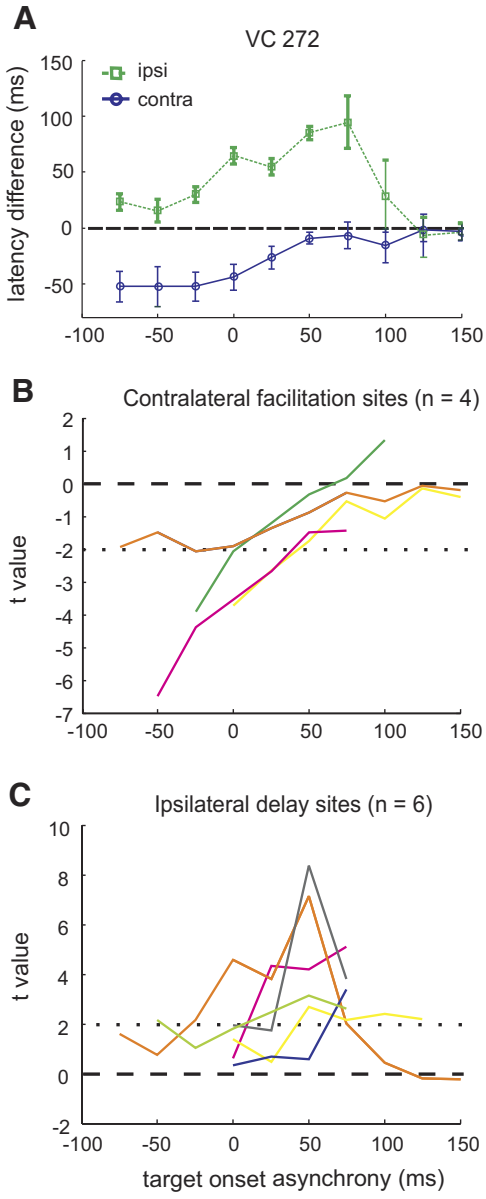

FIG. 5. The effect of varying TOAs. *A*: facilitation (blue circles) and delay (green squares) obtained with 65 μA at a single site (GU 26), with −75- to +150-ms TOAs. Error bars represent 95% confidence intervals of the mean difference between stimulated and control trials. *B*: data from all 4 facilitation sites with various TOAs; *t*-values indicate the magnitude of the latency difference between stimulated and control trials; the dotted line indicates the lower boundary for a 2-tailed *t*-test ($\alpha \leq 0.05$). *C*: data from 6 ipsilateral delay sites. Details as in *B*.

positive values to delay. Contralateral saccades were significantly facilitated as early as −75 ms; the effect dissipated at +50 ms. Ipsilateral saccades were delayed for most TOAs tested and delay was maximal with a +75-ms TOA. Figure 5*B* shows the effect of stimulating with different TOAs for four contralateral facilitation sites. The latency difference between control and stimulated trials is indicated by *t*-values and the dotted line shows the 95% confidence interval. Note that the facilitation effect dissipated for all four sites with later TOAs. Three of these sites were in the SEF. Figure 5*C* summarizes all six ipsilateral delay sites probed with different TOAs. Delay was not significant with a negative, −25-ms TOA, but positive ones produced delay that was maximal with TOAs of +50 and +75 ms. Overall, for all bilateral delay sites obtained with a +75-ms TOA (17 of 25 found in the pre-SMA), most of them (23 of 25) showed significant bilateral delay with a +75-ms TOA but no delay with a −25-ms TOA; only two sites showed significant ipsilateral but not contralateral delay with the −25-ms TOA.

Figure 6 shows the effect of manipulating stimulation amplitude on saccade delay with the TOA fixed at +75 ms and duration at 100 ms. Figure 6*A* shows the latency change at an example bilateral delay site (VC 270; depth = 3.5 mm, A/P = 2 mm, M/L = 3 mm), which was found with 50-μA current. This site was chosen because it showed a large effect and was tested with the full set of current amplitudes. Again, positive values are delays. Figure 6*B* shows horizontal eye traces obtained from the same site with different currents. As current amplitude was heightened, delay increased gradually for saccades in both directions, rather than being all or none (i.e., either delayed for the duration of stimulation or not at all). With larger-amplitude currents (>400 μA), saccades were delayed for longer than the stimulation duration of 100 ms. Figure 6*C* summarizes contralateral and ipsilateral effects separately for all five bilateral delay sites at which current amplitude was manipulated. Four of the five sites were located in the pre-SMA. In general, increasing current amplitude (20 to 500 μA) enhanced the delay effect proportionally.

Figure 7 shows the effect of manipulating stimulation duration on saccade delay with TOA set at +75 ms and current at 50–75 μA. In Fig. 7*A* are results obtained from a typical bilateral delay site (VC 285; depth = 2.4 mm, A/P = −1 mm, M/L = −2 mm). Figure 7*B* shows results for all current durations tested. Saccades in both directions were maximally delayed with 100-ms stimulation and the effect was not further increased with longer durations. The strong bilateral delay

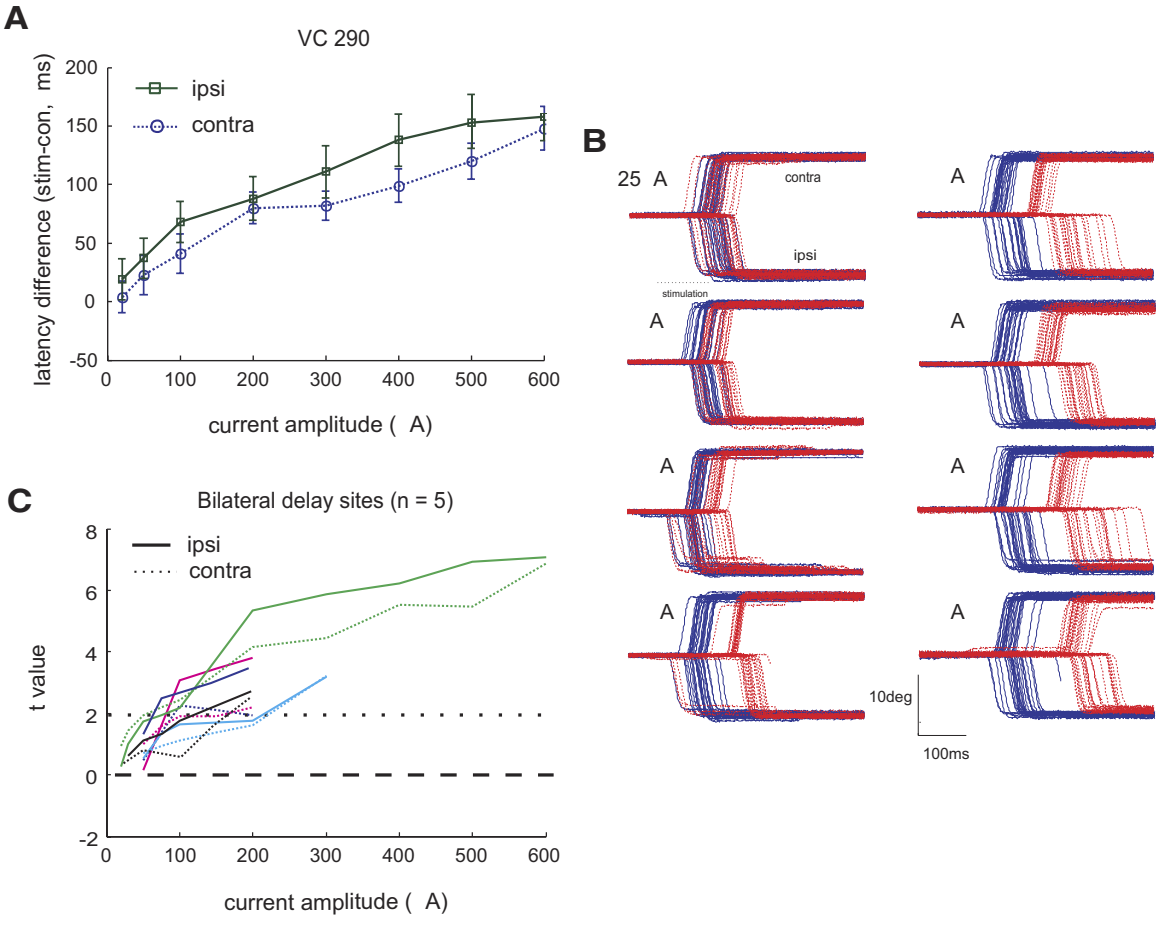

FIG. 6. The effect of varying current amplitude. *A*: delay elicited with 20- to 600-μA current from a single site (VC 292). Details as in Fig. 5. *B*: horizontal eye traces obtained with various current amplitudes from the same site as in *A*. *C*: data from 5 bilateral delay sites with various current amplitudes. Lines of the same color represent data from the same site (solid: contralateral; dashed: ipsilateral).

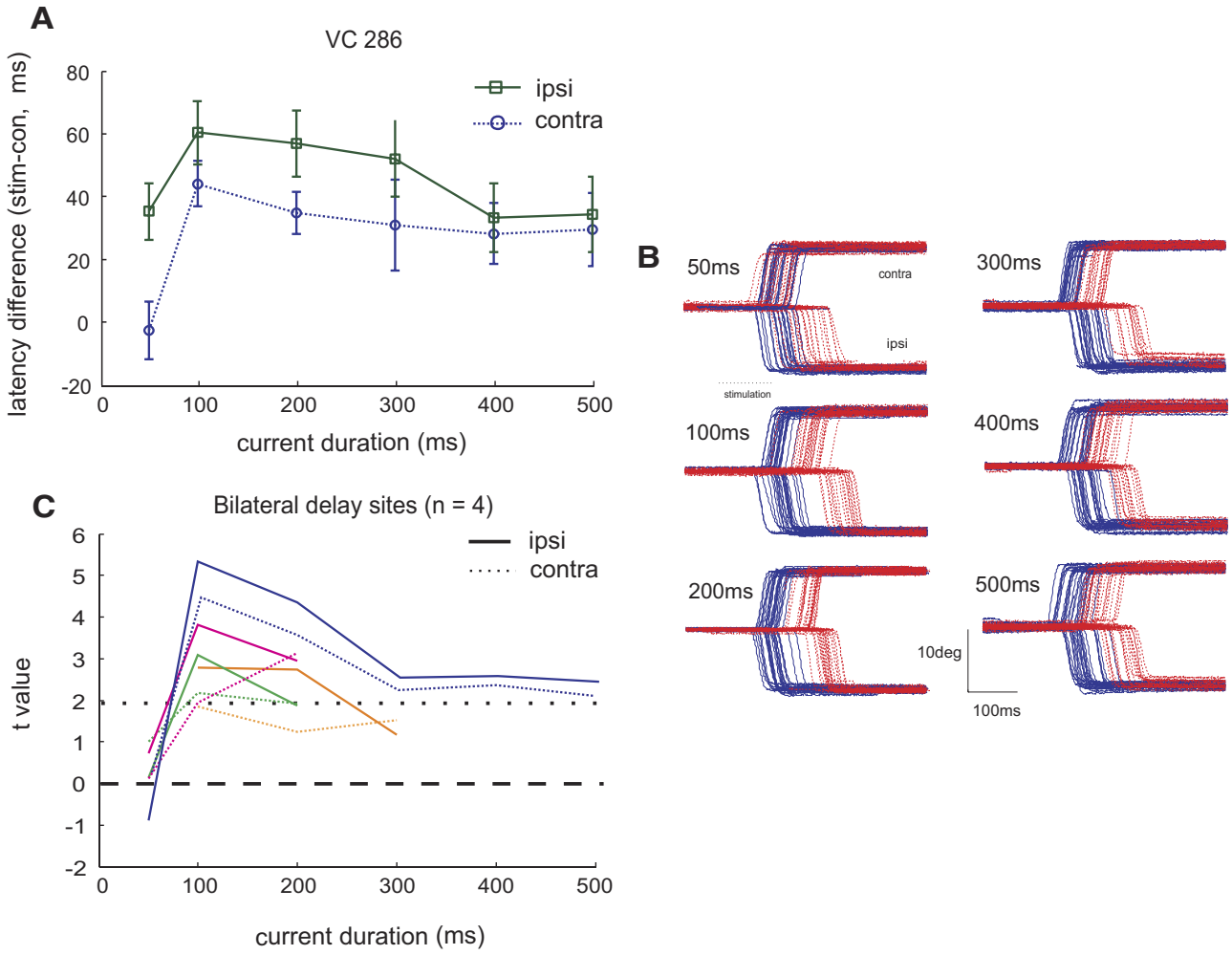

FIG. 7. The effect of varying current duration. *A*: effect of varying current duration obtained from an example site CL 87. Details as in Fig. 5. *B*: horizontal eye traces obtained with various current durations. *B*: data from 4 bilateral delay sites.

observed here indicates that a weak stimulation effect does not account for the lack of further increase in saccade delay with longer stimulation durations. Figure 7*C* summarizes the duration manipulation results for four bilateral delay sites. In general, increasing duration beyond 100 ms did not further increase delay.

We also manipulated current amplitude and duration at three contralateral facilitation sites with 50-, 100-, and 200-μA amplitudes or with 100-, 200-, and 500-ms durations (TOA = -25 ms). No significant differences in facilitation relative to those obtained with the 50- to 75-μA amplitude and 100-ms duration currents were observed (all $P > 0.05$). When these sites tested with +75-ms TOA and 50- to 200-μA current, a slight delay occurred for all current amplitudes, but it was not significantly different for different amplitudes (all $P > 0.05$).

Saccade metrics

Since Isoda (2004) reported that saccade metrics and dynamics were altered for delayed saccades at some pre-SMA stimulation sites, we examined whether this occurred in our data. Figure 8*A* shows horizontal and vertical eye position and Fig. 8*B* shows horizontal velocity recorded during stimulation at three sites. No differences were found in saccade endpoint, trajectory deviation, or peak velocity between control and stimulated trials for any of the three sites. Figure 8, *C–E* summarizes the results for all sites where a significant effect on saccade latency was observed. Figure 8*C* shows that only occasionally (12/108) did the stimulation produce a significant difference in endpoint error. Furthermore, the latency change was not correlated with the change in endpoint [delay sites: $r_{(91)} = -0.032$, $P = 0.717$; facilitation sites: $r_{(17)} = -0.337$, $P = 0.107$]. Figure 8, *D* and *E* shows that stimulation only infrequently altered maximal trajectory deviation and peak velocity as well (trajectory deviation: 8/108; peak velocity, 11/108). Again, no significant correlations between latency change and trajectory deviation were found [delay sites: $r_{(91)} = -0.033$, $P = 0.695$; facilitation sites: $r_{(17)} = -0.236$, $P = 0.302$], nor between latency and peak velocity change [delay sites: $r_{(91)} = -0.088$, $P = 0.584$; facilitation sites: $r_{(17)} = -0.209$, $P = 0.263$]. These results suggest that the main effect of stimulation was on saccade latency and not on the computation of saccade metrics or dynamics.

Spatial tuning of stimulation effects

To estimate the spatial extent of the latency effect, at 21 of the 79 significant sites, stimulation (50 or 75 μA) was given

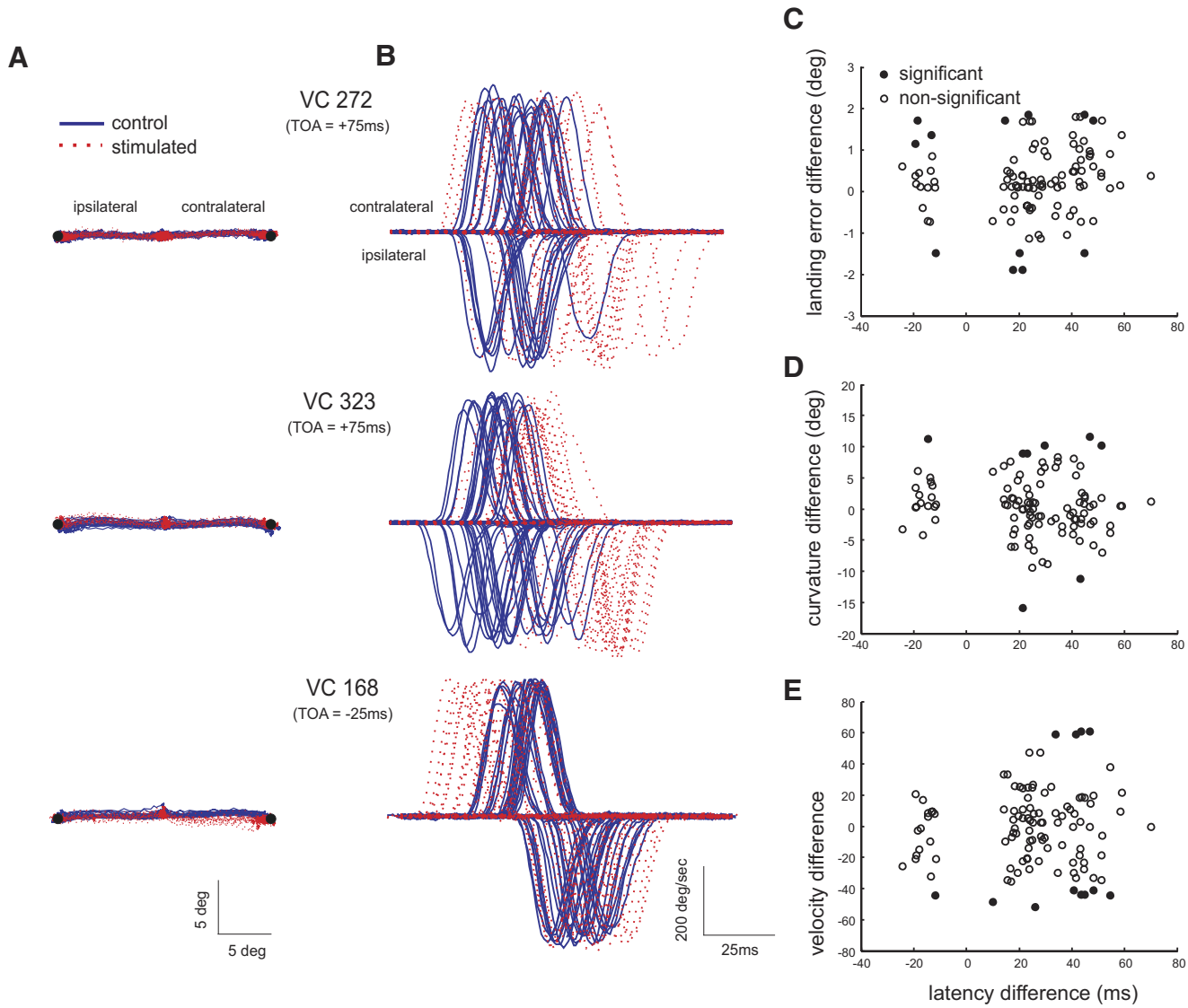

FIG. 8. Metrics and dynamics of control and stimulated saccades. *A*: horizontal and vertical eye positions for stimulated and control trials obtained from 3 example sites. *B*: horizontal eye velocity for the same trials. *C*: difference in saccade endpoint. Each point represents the mean difference in saccade endpoint error as a function of the mean latency change. Only sites with significant latency changes were included. A positive value indicates a larger landing error for stimulated trials. Significant differences are represented by filled circles ($P < 0.05$). *D*: difference in maximum trajectory deviation. Details as in *B*. *E*: difference in peak velocity.

while a saccade was being planned to a target randomly presented at one of 36 locations. Targets were displayed at 5, 10, or 15° eccentricity and in one of 12 directions spaced by 30° radial angles. A sufficient number of trials were obtained from four sites with a +75-ms TOA, two sites with a −25-ms TOA, and 15 sites with both −25- and +75-ms TOAs. A summary of the delay/facilitation results is shown in columns 6 and 7 of Table 1. Of the 19 sites where a +75-ms TOA was used, significant delay occurred for at least one target location at 14 sites and no sites produced facilitation. Of the 17 sites tested with a −25-ms TOA, significant facilitation was observed at one or more target locations at 9 sites. At 7 of these 9 sites, saccades were evoked with the same current amplitude when the monkey was in the dark.

Figure 9*A* shows three-dimensional maps of the latency change obtained at one site and from all 36 target locations with −25- (Fig. 9*A*, *top*) and +75-ms (Fig. 9*A*, *bottom*) TOAs. The axes represent horizontal and vertical target locations and the colors indicate the magnitude of latency change, where negative values represent facilitation. With a −25-ms TOA, saccades were facilitated in a limited contralateral region and moderately delayed in a broader, ipsilateral region. With +75-ms TOA, saccades were significantly delayed toward most locations, but more so ipsilateral to the stimulated site. Note that facilitation did not occur with the +75-ms TOA. Figure 9*B* shows maps constructed from a bilateral delay site (VC 169). With a −25-ms TOA, there was no significant delay at any target location. With a +75-ms TOA, saccades were significantly delayed toward most locations, but more so for ipsilateral than for contralateral ones.

To quantify the spatial tuning of the stimulation effect, we normalized the latency change at different target locations relative to the location with the maximum effect (see METHODS). The magnitudes of delay at locations of equal eccentricity

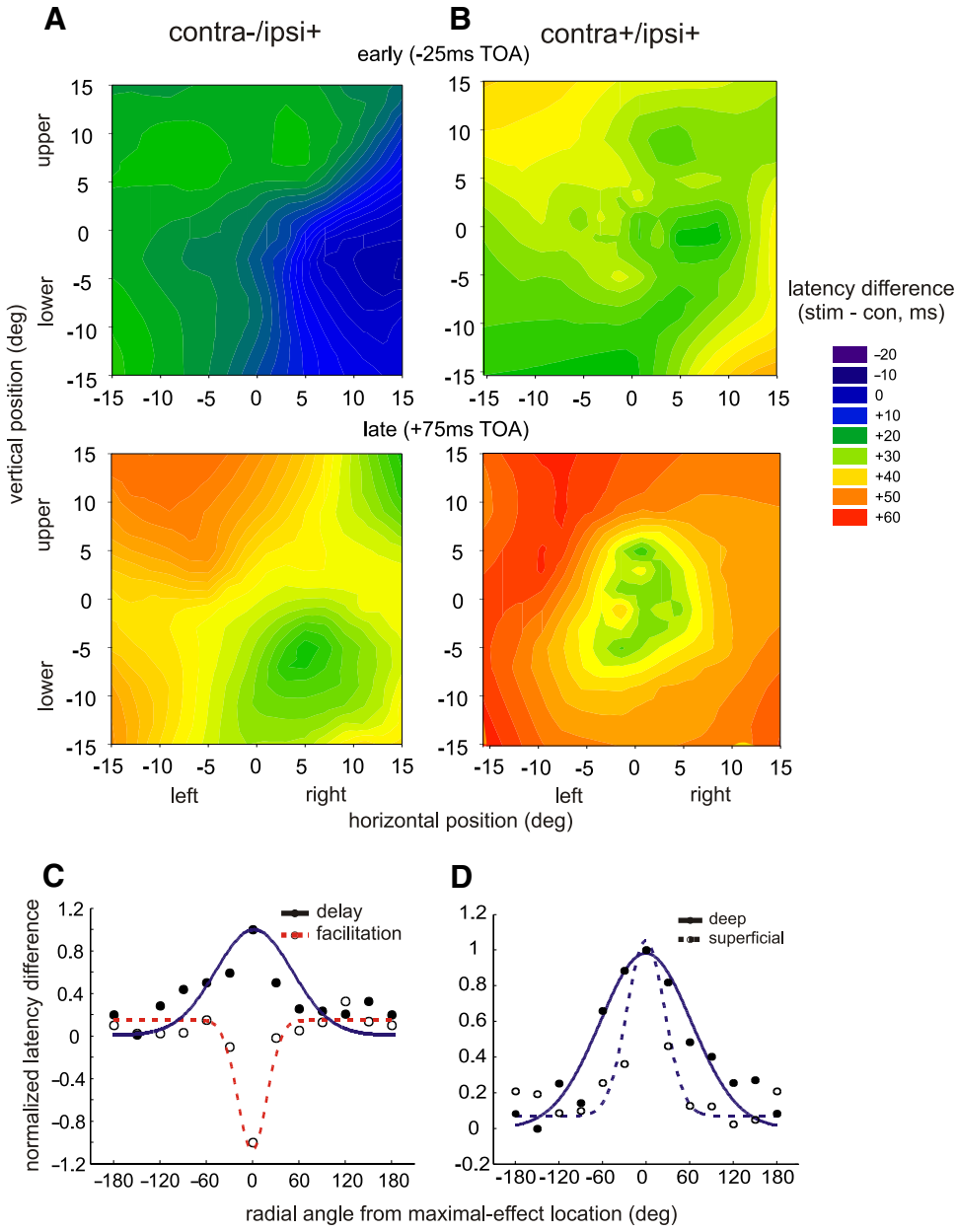

FIG. 9. Spatial tuning of saccade delay and facilitation. *A*: maps of latency change when stimulation was delivered with a −25- (*top*) or a +75-ms (*bottom*) TOA, from a contralateral facilitation site. The *x*-axis represents horizontal target position (negative indicates left) and the *y*-axis vertical. Stimulation effect magnitude is represented by color; negative numbers are facilitation. The map was constructed using a Loess smooth function (0.4 sampling proportion and one polynomial degree). *B*: maps of latency change when stimulation was delivered with a −25- (*top*) or a +75-ms (*bottom*) TOA, obtained from a bilateral delay site. *C*: directional tuning curves of facilitation (red curve) and delay effects (blue curve). Each data point represents the normalized latency difference (filled circles: delay sites, $n = 14$; open circles: facilitation sites, $n = 9$). For each site, the angle of the maximum latency difference was determined; latency differences for other angles of the same eccentricity were normalized to it. *D*: directional tuning of the delay effect at 8 superficial (open circles, $n = 8$) and 6 deep (filled circles, $n = 6$) sites. Details as in *C*.

relative to the location of maximal delay effect were first aligned angularly by placing the maximum effect location at 0° and the adjacent locations at their respective relative angles (e.g., −30 and +30°). The magnitude of the latency change for the adjacent locations was then normalized to that of the maximum delay location. This procedure was performed for all 14 delay sites where the +75-ms TOA was used, after which the resulting normalized scores were then averaged. The same procedure was applied to the 9 facilitation sites where the −25-ms TOA was used. Figure 9*C* show the normalized mean latency differences for the delay (filled circles) and facilitation sites (open circles) and the corresponding Gaussian-fitted curves (see METHODS). Here, each point represents the average of the normalized scores of the same realigned angles across all sites. When the variance of the Gaussian-fitted curves was compared, the delay effect was more broadly tuned than the facilitation effect [$F(12,12) = 4.00$, $P < 0.01$].

To compare the spatial tuning of delay for superficial and deep sites, the 14 sites were divided into two groups based on their depth (superficial sites: <2 mm, mean depth = 1.5 mm, $n = 8$; deep sites: ≥2 mm, mean depth = 2.4 mm, $n = 6$), and the same procedure was used to compute the normalized scores for the two groups. Figure 9*D* shows the resulting scores and Gaussian-fitted curves. The Gaussian of the superficial delay sites had a significantly smaller variance than that of the deeper ones [$F(12,12) = 2.42$, $P < 0.05$]. In summary, facilitation was usually contralateral, narrowly tuned, and elicited with a −25-ms TOA. Delay on the other hand was usually stronger ipsilaterally, broadly tuned, and occurred with a +75-ms TOA. In addition, tuning for deeper delay sites was broader than that at superficial ones.

Evoked saccades at facilitation sites in the present study converged to a limited contralateral area, as some studies have shown in the past (Park et al. 2005; Tehovnik and Lee 1993).

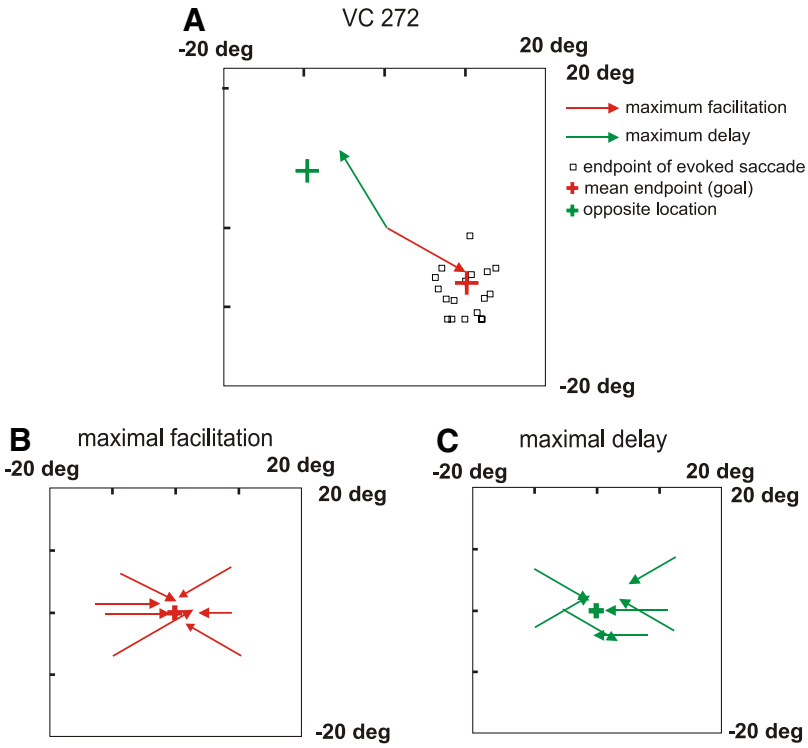

FIG. 10. Relationship between the goal of evoked saccades and the target locations of maximally delayed and facilitated saccades at the same sites. *A*: an example of endpoints of evoked saccades and the target locations of maximally facilitated and delayed saccades, recorded from site VC 272. *B*: vectors of target locations for maximally facilitated saccades in relation to the goal of evoked saccades for each facilitation site with a −25-ms TOA ($n = 7$). *C*: vectors of target locations for maximally delayed saccades in relation to the opposite location of the goal of evoked saccades for the same sites with a −25-ms TOA.

If saccade facilitation relies on the same signal for evoking saccades, their topography should be consistent with each other. To examine this, we computed the goal (mean endpoint) of evoked saccades for the facilitation site and compared it to the target locations at which the maximum facilitation and delay were found at the same site. Figure 10*A* shows the target location to which maximum facilitation occurred with a −25-ms TOA (red arrow), the target location to which maximal delay occurred with a +75-ms TOA (green arrow), and the endpoints of saccades evoked at the same site (squares). The goal of evoked saccades is indicated by the red cross and the opposite location by the green cross. Note that the goal of evoked saccades is consistent with the target location where maximum facilitation was observed.

To summarize these data, the metrics of the target location where maximum saccade facilitation occurred for each site were plotted relative to the goal of saccades evoked at that site. Figure 10*B* shows that for the seven sites where both facilitation and evoked saccades were obtained, the goal of the evoked saccades was consistently close to the target location of the facilitated saccades. Conversely, Fig. 10*C* shows that the target location of delayed saccades was near the opposite location of the evoked saccade goal. Therefore saccades directed toward locations consistent with the goal of evoked saccades were usually facilitated and those directed away from the goal were usually maximally delayed.

DISCUSSION

The present study reveals three important differences between the SEF and the pre-SMA that could elucidate their roles in saccade selection. First, the stimulation effect found at and close to the SEF is spatially tuned, in that visually guided saccades to target locations consistent with the goal of evoked saccades are facilitated and those directed away from it are maximally delayed. In contrast, stimulation at and close to the pre-SMA usually delays saccades bilaterally. Second, the latency change that occurs following stimulation to either structure depends on when the current is delivered. Stimulating the SEF produces maximum facilitation when given before target onset (see Fig. 5). In both the SEF and pre-SMA, stimulation is more likely to produce delay when administered after target onset (see Table 1). Finally, elevating current amplitude increases bilateral delay in the pre-SMA, but does not significantly change the latency of contralateral facilitation and ipsilateral delay in the SEF.

Note that in the present study facilitation sites were not all located within the SEF and bilateral delay sites were not all located in the pre-SMA; moreover, the type of sites found near the boundary of these two regions was mixed. Consistent with this, Isoda (2004) observed both bilateral delay and facilitation in the pre-SMA. Therefore it is likely that the transition from one type of sites to the other is gradual rather than abrupt.

Previous research distinguished the SEF and the pre-SMA based on their roles in saccade planning (Fujii et al. 2002) and in resolving competing voluntary saccade plans (Nachev et al. 2005), but not in saccade target selection. In them, the activity of SEF neurons appears to specify saccadic movements more than that of pre-SMA neurons (Fujii et al. 2002) and the rostral pre-SMA seems more involved in resolving conflict between voluntary saccade plans, whereas the SEF appears involved in successfully selecting a saccade target (Nachev et al. 2005). Our findings are consistent with these and, further, implicate both structures in playing different roles in saccade selection.

Our results are consistent with the hypothesis that the SEF is involved in selecting a specific saccade and that stimulation here likely activates a subthreshold endogenous command that facilitates the selected saccade. Facilitation might occur through an interaction of the SEF output with visually guided

saccade planning in downstream structures to which it projects, such as the FEF or SC. Because the command is subthreshold, it does not directly trigger a saccade; rather, it shortens saccade latency when the target location and the preferred location of the SEF saccade command are consistent. The same stimulation could selectively delay a saccade to a target in a location different from that of the SEF endogenous movement command. Under this scheme, when selection of one from multiple saccade targets is required (McPeek and Keller 2002, 2004; Walker et al. 1994, 1997), the SEF could influence the selection.

In a recent study, SEF stimulation during a countermanding task resulted in saccade delay with a current amplitude lower than ours, but no facilitation was found (Stuphorn and Schall 2006). The absence of facilitation effect in their study is not surprising because we found that facilitation sites are relatively infrequent and depend critically on target location. Furthermore, stimulation produces the greatest amount of facilitation when given before target onset, but it was delivered after target onset in their countermanding experiment, possibly too late to cause an effect. Another potential reason that facilitation was not seen in that study is that the context of the countermanding paradigm, which resulted in longer saccade latency in general (as reported in Stuphorn and Schall 2006), might increase the level of fixation activity in visuomotor structures in both go and no-go trials. As a result, the threshold for stimulation-induced facilitation could have been elevated and the amount of current needed for generating delay would have been lower.

Our findings support the hypothesis that the pre-SMA is not directly involved in selecting a specific saccade but in delaying currently planned ones, consistent with its lack of direct connections to the SC and brain stem. Instead, it might influence saccade selection by delaying saccades bilaterally via other cortical or subcortical regions with which it has direct connections, such as the FEF (Huerta and Kaas 1990; Luppino et al. 1993). The pre-SMA might modulate fixation activity in the FEF to control the amount of delay, thereby allowing the preferred saccade to be selected by other structures, such as the SEF. Similar modulation of saccade latency by fixation signals has been suggested in recent computational and physiological work on saccade initiation times (e.g., Carpenter and Williams 1994; Schall and Hanes 1996).

Another study of the pre-SMA arrived at a different conclusion about this area's role in saccade selection (Isoda and Hikosaka 2007), in which, when a cue changed color to signal a switch in the desired direction of a planned saccade, neurons here were more active for switched saccades than for saccades in the same direction without a switch. Based on these results, the authors suggested that the pre-SMA facilitates saccades to preferred locations and suppresses saccades to nonpreferred ones. However, their study also showed that stimulating the pre-SMA in a go/no-go paradigm, although improving performance in the task, delayed saccades made in both go and no-go trials. This result is inconsistent with the idea that the pre-SMA facilitates saccade initiation, but rather supports our interpretation that neurons here suppress an unwanted saccade to allow a desired one to be selected by another structure such as the SEF.

Finally, with respect to the effect of stimulation timing, our findings suggest that current applied to the SEF must be delivered well before movement onset to reliably facilitate saccades. Early SEF stimulation may be necessary to affect saccade planning in other structures, given the long latency for evoking saccades from the SEF. In contrast, SEF stimulation delays saccades when delivered after target onset but before saccade initiation and its effect dissipates shortly after the end of stimulation, likely by directly activating spatially selective fixation neurons downstream. Pre-SMA stimulation, which also required later TOAs to delay saccades, could directly activate nonselective fixation neurons downstream. These two regions might have access to spatially selective or nonselective fixation neurons, respectively, such as those found in the FEF (Sommer and Wurtz 2000). In contrast with our results, an earlier study reported that SEF stimulation also resulted in bilateral suppression of FEF movement neurons (Sadeghpour et al. 1998). The discrepancy between their results and ours can be reconciled if their stimulation actually activated bilateral delay sites in the DMFC.

ACKNOWLEDGMENTS

We thank J. Badler and H. Hwang for assistance on statistical analysis and software preparation.

GRANTS

This work was supported by National Eye Institute Grant EY-11720 to S. Heinen and an R. C. Atkinson fellowship to S.-n. Yang.

REFERENCES

Amador N, Schlag-Rey M, Schlag J. Primate antisaccade. II. Supplementary eye field neuronal activity predicts correct performance. *J Neurophysiol* 91: 1672–1689, 2004.

Arai K, Keller EL. A model of the saccade-generating system that accounts for trajectory variations produced by competing visual stimuli. *Biol Cybern* 92: 21–37, 2005.

Arai K, Keller EL, Edelman JA. Two-dimensional neural network model of the primate saccadic system. *Neural Networks* 7: 1115–1135, 1994.

Basso MA, Wurtz RH. Neuronal activity in substantia nigra pars reticularta during target selection. *J Neurosci* 22: 1883–1894, 2002.

Carpenter RHS, Williams MLL. Neural computation of log likelihood in control of saccadic eye movements. *Nature* 377: 59–62, 1995.

Findlay JM, Walker R. A model of saccade generation based on parallel processing and competitive inhibition. *Behav Brain Sci* 22: 661–674, 1999.

Fries W. Inputs from motor and premotor cortex to the superior colliculus of the macaque monkey. *Behav Brain Res* 18: 95–105, 1985.

Fujii N, Mushiake H, Tanji J. Distribution of eye- and arm-movement-related neuronal activity in the SEF and in the SMA and pre-SMA of monkeys. *J Neurophysiol* 87: 2158–2166, 2002.

Hartmann-von Monakow K, Akert K, Künzle H. Projections of precentral and premotor cortex to the red nucleus and other midbrain areas in Macaca fascicularis. *Exp Brain Res* 34: 91–105, 1979.

Hoshi E, Tanji J. Differential roles of neuronal activity in the supplementary and presupplementary motor areas: from information retrieval to motor planning and execution. *J Neurophysiol* 92: 3482–3499, 2004.

Huerta MF, Kaas JH. Supplementary eye field as defined by intracortical microstimulation: connections in macaques. *J Comp Neurol* 293: 299–330, 1990.

Isoda M. Context-dependent stimulation effects on saccade initiation in the presupplementary motor area of the monkey. *J Neurophysiol* 93: 3016–3022, 2004.

Isoda M, Hikosaka O. Switching from automatic to controlled action by monkey medial frontal cortex. *Nat Neurosci* 10: 240–248, 2007.

Isoda M, Tanji J. Cellular activity in the supplementary eye field during sequential performance of multiple saccades. *J Neurophysiol* 88: 3541–3545, 2002.

Isoda M, Tanji J. Participation of the primate presupplementary motor area in sequencing multiple saccades. *J Neurophysiol* 92: 653–659, 2004.

Judge SJ, Richmond BJ, Chu FC. Implantation of magnetic search coils for measurement of eye position: an improved method. *Vision Res* 20: 535–538, 1980.

Leigh RJ, Zee DS. *The Neurology of Eye Movements.* New York: Oxford Univ. Press, 2006.

Li X, Basso M. Competitive stimulus interactions within single response fields of superior colliculus neurons. *J Neurosci* 25: 1357–1373, 2005.

Lu X, Matsuzawa M, Hikosaka O. A neural correlate of oculomotor sequences in supplementary eye field. *Neuron* 34: 317–325, 2002.

Luppino G, Matelli M, Camarda R, Rizzolatti G. Corticocortical connections of area F3 (SMA-proper) and area F6 (pre-SMA) in the macaque monkey. *J Comp Neurol* 338: 114–140, 1993.

Martinez-Trujillo JC, Wang H, Crawford JD. Electrical stimulation of the supplementary eye fields in the head-free macaque evokes kinematically normal gaze shifts. *J Neurophysiol* 89: 2961–2974, 2003.

McPeek RM, Keller EL. Superior colliculus activity related to concurrent processing of saccade goals in a visual search task. *J Neurophysiol* 87: 1805–1815, 2002.

McPeek RM, Keller EL. Deficits in saccade target selection after inactivation of superior colliculus. *Nat Neurosci* 7: 757–763, 2004.

Missal M, Heinen SJ. Facilitation of smooth pursuit initiation by electrical stimulation in the supplementary eye fields. *J Neurophysiol* 86: 2413–2425, 2001.

Nachev P, Rees G, Parton A, Kennard C, Husain M. Volition and conflict in human medial frontal cortex. *Curr Biol* 15: 122–128, 2005.

Park J, Schalg-Rey M, Schlag J. Frames of reference for saccadic command tested by saccade collision in the supplementary eye field. *J Neurophysiol* 95: 159–170, 2005.

Russo GS, Bruce CJ. Supplementary eye field: representation of saccades and relationship between neural response fields and elicited eye movements. *J Neurophysiol* 84: 2605–2621, 2000.

Sadeghpour S, Schlag J, Schlag-Rey M, Mohempour A, Dorfman A. Functional interactions between the supplementary and frontal eye fields in monkey. *Soc Neurosci Abstr* 24: 522, 1998.

Schall JD. Neuronal activity related to visually guided saccadic eye movements in the supplementary motor area of Rhesus monkeys. *J Neurophysiol* 66: 530–558, 1991.

Schall JD, Stuphorn V, Brown JW. Monitoring and control of action by the frontal lobes. *Neuron* 36: 309–322, 2002.

Schiller PH, Chou I. The effects of frontal eye field and dorsomedial frontal cortex lesions on visually guided eye movements. *Nat Neurosci* 1: 248–253, 1998.

Schlag J, Schlag-Rey M. Evidence for a supplementary eye field. *J Neurophysiol* 57: 179–200, 1987.

Schlag-Rey M, Amador N, Sanchez H, Schlag J. Antisaccade performance predicted by neuronal activity in the supplementary eye field. *Nature* 390: 398–401, 1997.

Shook BL, Schlag-Rey M, Schlag J. Direct projection from the supplementary eye field to the nucleus raphé interpositus. *Exp Brain Res* 73: 215–218, 1988.

Shook BL, Schlag-Rey M, Schlag J. Primate supplementary eye field: I. Comparative aspects of mesencephalic and pontine connections. *J Comp Neurol* 301: 618–642, 1990.

Sommer MA, Wurtz RH. Composition and topographic organization of signals sent from the frontal eye field to the superior colliculus. *J Neurophysiol* 83: 1979–2001, 2000.

Stuphorn V, Schall JD. Executive control of countermanding saccades by the supplementary eye field. *Nat Neurosci* 9: 925–931, 2006.

Stuphorn V, Taylor TL, Schall JD. Performance monitoring by the supplementary eye field. *Nature* 408: 857–860, 2000.

Tanji J. Sequential organization of multiple movements: involvement of cortical motor areas. *Annu Rev Neurosci* 24: 631–651, 2001.

Tehovnik EJ. The dorsomedial frontal cortex: eye and forelimb fields. *Behav Brain Res* 67: 147–163, 1995.

Tehovnik EJ, Lee K. The dorsomedial frontal cortex of the rhesus monkey: topographic representation of saccades evoked by electrical stimulation. *Exp Brain Res* 96: 430–442, 1993.

Tehovnik EJ, Lee K, Schiller PH. Stimulation-evoked saccades from the dorsomedial frontal cortex of the rhesus monkey following lesions of the frontal eye fields and superior colliculus. *Exp Brain Res* 98: 179–190, 1994.

Tehovnik EJ, Sommer MA. Electrically evoked saccades from the dorsomedial frontal cortex and frontal eye fields: a parametric evaluation reveals differences between areas. *Exp Brain Res* 117: 369–378, 1997.

Thompson KG, Hanes DP, Bichot NP, Schall JD. Perceptual and motor processing stages identified in the activity of macaque frontal eye field neurons during visual search. *J Neurophysiol* 76: 4040–4055, 1996.

Tolias AS, Sultan F, Augath M, Oeltermann A, Tehovnik EJ, Schiller PH, Logothetis NK. Mapping cortical activity elicited with electrical microstimulation using fMRI in the macaque. *Neuron* 48: 901–911, 2005.

Trappenberg TP, Dorris MC, Munoz DP, Klein RM. A model of saccade initiation based on the competitive integration of exogenous and endogenous signals in the superior colliculus. *J Cogn Neurosci* 13: 256–271, 2001.

Walker R, Deubel H, Schneider WX, Findlay JM. Effect of remote distractors on saccade programming: evidence for an extended fixation zone. *J Neurophysiol* 78: 1108–1119, 1997.

Walker R, Kentridge RW, Findlay JM. Independent contributions of the orienting of attention, fixation offset and bilateral stimulation on human saccadic latency. *Exp Brain Res* 103: 294–310, 1995.

Wurtz RH, Goldberg ME. *The Neurobiology of Saccadic Eye Movements.* Amsterdam: Elsevier Science, 1989.